

## Analysis of the electronic properties of extremely condensed matter by the discrete-variational $X\alpha$ method: Application to cold dense neon plasma

Kazumi Fujima and Tsutomu Watanabe

*The Institute of Physical and Chemical Research (RIKEN), Wako, Saitama 351-01, Japan*

Hirohiko Adachi

*The Hyogo University of Teacher Education, Yashiro-cho, Kato-gun, Hyogo 673-14, Japan*

(Received 4 January 1984; revised manuscript received 21 June 1985)

To investigate dense matter the discrete-variational  $X\alpha$  method is applied to neon clusters to calculate their energy levels. In these clusters atoms are assumed to be located at simple or face-centered cubic sites. The calculations are carried out up to a density of about 1000 times that of a usual solid. For highly compressed clusters the kinetic energies of orbitals, as well as the repulsive potentials between electrons, increase. At the same time attractive potentials between electrons and neighboring nuclei lower the energies. As a result of these two competitive effects, orbital energies do not change monotonically with the density.

### I. INTRODUCTION

Extremely dense plasma, whose density is a few hundred times that of a usual solid, can be produced nowadays in the inertial-confinement fusion experiments. In these experiments the plasma temperature is thought to be over hundreds of electron volts. This experimental progress has prompted many theoretical studies of its electronic property based on various models. These models are usually characterized by the so-called ion-coupling parameter  $\Gamma$  introduced by Brush *et al.*<sup>1</sup> It is defined as the ratio of the repulsive potential energy  $(eZ^*)^2/R_0$  between a pair of ions with an effective charge  $eZ^*$  and separated at a distance  $R_0$  to the kinetic energy  $k_B T$  of the thermal motion of the ions [i.e.,  $\Gamma = (eZ^*)^2/R_0 k_B T$ ].

The electronic states of a low-density and high-temperature plasma (i.e.,  $\Gamma < 1$ ) can be treated as atomic. Neighboring ions and electrons outside the ion core change the electronic potential and they affect orbital energies. Various methods are proposed to find this effective potential and the electronic states in it.<sup>2-5</sup> These levels are also subject to Stark broadening by the strong electronic field of the surrounding ions.

When  $\Gamma$  exceeds unity, atoms in the plasma come into close physical proximity and the atomic orbitals encounter the neighboring atoms. For a sufficiently dense plasma the Debye length is nearly equal to the ion-sphere radius. The ion-sphere model and the Thomas-Fermi theory as well as its modifications are most frequently used in this density region.<sup>6</sup> Within the atomic picture the behavior of the compressed electrons can be solved without much difficulty.

However, these atomic models cannot take into account the covalent nature between atoms. Solid-state physics can provide alternative approaches. For example, an extension of the tight-binding approximation for disordered material<sup>7</sup> has produced fruitful results. However, it works only in limited density or temperature regions.

Here in this paper we report a cluster approach using the discrete-variational  $X\alpha$  method (referred to as the

DV- $X\alpha$  method, hereafter). The DV- $X\alpha$  method has been applied so far to the analysis of chemical bonding, the estimation of optical transition energies, and so on. It has proved to give accurate one-electron orbital energies for many materials. A relativistic version of this method has been also used for the analysis of quasimolecular x rays.<sup>8</sup> There the situation is similar to our present problem in the sense that the nuclei are located close to each other.

The DV- $X\alpha$  method has three advantages. First, this method allows us to go beyond the atomic picture; electronic levels can be obtained in the molecular scheme, and the results will show not only a shift from atomic levels but also splitting into bands of levels. The lowest edge of the bands may give information on the so-called continuum lowering. Second, the DV- $X\alpha$  method uses numerical basis functions generated from an atomic effective potential in the cluster, which, in turn, is determined by the wave function of the cluster. The effective potential and the wave function are calculated in a self-consistent manner. This procedure reduces the computational effort as compared with the usual self-consistent Hartree-Fock method. Third, the muffin-tin potential approximation is unnecessary. The DV- $X\alpha$  method allows us an accurate estimation of orbital energies.

In this report the DV- $X\alpha$  method is applied to neon clusters in which the motion of the nuclei is assumed to be frozen. Since the electrons move much faster than the nuclei, this assumption is justified as a first-step approach. Neon is used frequently in inertial-confinement experiments.<sup>9</sup> We discuss here only those features of electronic properties which are common to all cluster types, because the nuclear configuration is fixed in a somewhat arbitrary way as explained in the next paragraph. The densities, up to about 1000 times that of a usual solid, are treated here. The highest of densities has not yet been achieved experimentally. Knowledge of this density region may be useful for the analysis of future experimental data.

The results of a computational simulation<sup>10</sup> show a

sharp peak in the correlation function of ions in the plasma in the high-density limit. Since this suggests a short-range order for the configuration of ions, they are packed closely, at least, for a sufficiently dense plasma. Therefore, we take up here two types of model clusters, i.e., a simple cubic  $\text{Ne}_8$  cluster and a face-centered-cubic  $\text{Ne}_{13}$  cluster, which are buried in the neon matrix. The difference between the isolated clusters and those in the matrix is in the boundary conditions on the cluster. For an isolated cluster, the electronic wave function spreads out and is zero at infinity. For an embedded cluster, however, the electronic charges should maintain neutrality with the nuclear charge within a finite volume. Having this in mind, we have used boundary conditions specified in Secs. II and III B.

The plan of this paper is as follows. In Sec. II we review briefly the computational method of DV- $X\alpha$  and mention the points which are particularly important for the simulation of dense matter. In Sec. III A the results for the compressed atomic neon are presented. They are compared in Secs. III B and III C with the results for  $\text{Ne}_8$  and those for  $\text{Ne}_{13}$ . In Sec. IV the physical meaning of the results are discussed in detail. In Sec. V the unsolved problems in this work will be pointed out.

## II. COMPUTATIONAL METHOD

Since the detailed computational method is reported by Adachi and Rosen,<sup>11,12</sup> a brief review suffices here. In the DV- $X\alpha$  method single-electron states are calculated on the basis of an effective potential which involves the exchange interaction between electrons approximately in the form of a local potential proportional to the cubic root of the local density  $\rho(r)$  at each point  $r$ . We use atomic units unless otherwise noted.

The basis atomic radial wave functions  $R_{n,l}^v(r_v)$  with  $r_v = |r - R_v|$  in a spherical effective potential  $V_v$  are determined numerically by the Hartree-Fock-Slater (HFS) equation:

$$\left[ -\frac{1}{r_v^2} \frac{d}{dr_v} r_v^2 \frac{d}{dr_v} + 2V_v(r_v) + \frac{l(l+1)}{r_v^2} \right] R_{n,l}^v(r_v) = \epsilon_{n,l}^v R_{n,l}^v(r_v), \quad (2.1)$$

where  $n$  and  $l$  represent the usual principal and azimuthal quantum numbers. The effective atomic potential  $V_v(r_v)$  is given as the sum of the Coulomb potential  $V_C$  and the exchange potential  $V_{\text{ex}}$ :

$$V_v(r_v) = \begin{cases} V_{C,v}(r_v) + V_{\text{ex},v}(r_v) & \text{for } r_v \leq R_{\text{well}} \\ +\infty & \text{for } r_v > R_{\text{well}} \end{cases} \quad (2.2)$$

The radius  $R_{\text{well}}$  of the well potential will be discussed later. In Eq. (2.2)  $V_{C,v}$  is the sum of the attractive Coulomb potential from the nucleus of a charge  $Z_v$  and the repulsive Coulomb interaction between electrons, i.e.,

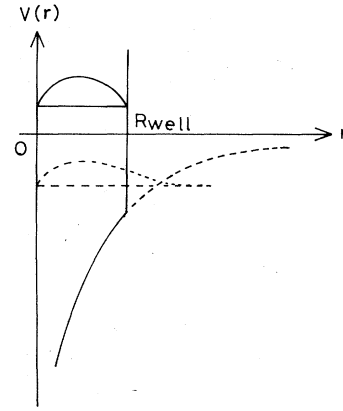


FIG. 1. The contribution of the well potential in Eq. (2.2) is schematically illustrated. Dotted and solid curves represent original and modified potentials and wave functions, respectively. The well potential truncates the tail of a wave function and consequently raises the kinetic energy of the orbital.

$$V_{C,v}(r_v) = -\frac{Z_v}{r_v} + \frac{1}{r_v} \int_0^{r_v} 4\pi r'^2 \rho_v(r') dr' + \int_{r_v}^{\infty} 4\pi r'^2 \frac{\rho_v(r')}{r'} dr', \quad (2.3)$$

where  $\rho_v$  is a spherical charge distribution around the  $v$ th nucleus. The exchange interaction  $V_{\text{ex},v}$  is given in the  $X\alpha$  approximation<sup>13</sup>

$$V_{\text{ex},v}(r_v) = -6\alpha \left[ \frac{3}{4\pi} \rho_v(r_v) \right]^{1/3}. \quad (2.4)$$

The parameter  $\alpha$  is fixed to be 0.7 for all of the calculations.

The effective potential outside  $R_{\text{well}}$  is assumed to be infinite in Eq. (2.2). In other words, a spherical well potential of radius  $R_{\text{well}}$  (called the well radius, hereafter) is superposed artificially on the effective atomic potential (see Fig. 1). This potential barrier is used to truncate the tail of the basis function in the usual application. In this work, this well potential can play the role of confining the basis function within a limited volume at the outset. The well radius is chosen so that charge neutrality is satisfied for a specified atomic or electron density.

The potential (2.3) is an atomic potential. The basis functions obtained using this potential are convenient for many practical purposes. At small interatomic distances, however, inner-core orbitals are extremely localized because of the attractive potential from the neighboring nuclei. These localized orbitals cannot be represented by linear combinations of the basis functions generated from the potential (2.3). Therefore, we take approximate account of the potential due to neighboring atoms by spherically averaging them, and use an effective potential

$$V_{C,v}(r_v) = -\frac{Z_v}{r_v} + \frac{1}{r_v} \int_0^{r_v} 4\pi r'^2 \rho_v(r') dr' + \int_{r_v}^{\infty} 4\pi r'^2 \frac{\rho_v(r')}{r'} dr' + \sum_{j \neq v} \left[ -\frac{Z_j}{|r_v - a_j|} + \frac{1}{2a_j r_v} \int_{r_v + a_j}^{|r_v - a_j|} r' \rho_j(r') dr' \right] \quad (2.5)$$

throughout the present calculations.  $a_j$  is the distance from  $r_v$  to  $j$ th atom.

The total Hamiltonian of the  $N$ -electron cluster is given by the sum of the kinetic energies and Coulomb and exchange terms as

$$H = -\frac{1}{2} \sum_{j=1}^N \nabla_j^2 + U_C + U_{ex} . \quad (2.6)$$

The Coulomb term  $U_C$  is calculated by gathering up the contributions from all atoms in the cluster, i.e.,

$$U_C = \begin{cases} \sum_v \left[ -\frac{Z_v}{r_v} + \frac{1}{r_v} \int_0^{r_v} 4\pi r'^2 \rho_v(r') dr' + \int_{r_v}^{\infty} 4\pi r'^2 \frac{\rho_v(r')}{r'} dr' \right] & \text{inside the cluster} \\ + \infty & \text{outside the cluster} . \end{cases} \quad (2.7)$$

(A precise definition of the cluster region will be given later.) The exchange term  $U_{ex}$  is given in the framework of the  $X\alpha$  approximation as

$$U_{ex} = -6\alpha \left[ \frac{3}{4\pi} \sum_n^N \rho_n(r) \right]^{1/3} . \quad (2.8)$$

Because the basis atomic wave functions prepared in Eq. (2.1) automatically satisfy the boundary condition on the surface of the potential wells, the separation of the cluster domain is not necessary. The role of these well potentials is considered in Sec. III.

The solution  $\psi$  of the Hamiltonian is expressed as a superposition of symmetrized orbitals  $\chi_j$ :

$$\psi(r) = \sum_j C_j \chi_j(r) . \quad (2.9)$$

Here the  $\chi_j$  are linear combinations of atomic basis functions, namely,

$$\chi_j = \sum_{\mu} W_{\mu}^j \phi_{\mu} = \sum_{\mu} W_{\mu}^j R_{n,\mu}^i(r) Y(\theta_{\mu}, \phi_{\mu}) . \quad (2.10)$$

The coefficients  $W_{\mu}^i$  are determined from the geometrical symmetry of the cluster.

A variational procedure leads to a secular equation,

$$HC = \epsilon SC \quad (2.11)$$

for vector  $C$ , whose elements are  $C_j$  in Eq. (2.9). Here  $H$  and  $S$  denote the Hamiltonian and overlap matrices defined by the elements

$$H_{ij} = \langle \chi_i | H | \chi_j \rangle \quad (2.12)$$

and

$$S_{ij} = \langle \chi_i | \chi_j \rangle . \quad (2.13)$$

In order to get the values of  $H_{ij}$  and  $S_{ij}$  the DV- $X\alpha$  method performs the integration using Diophantine-type integration.

Trial charge distributions  $\rho_v(r_v)$  for use in Eqs. (2.5), (2.7), and (2.8) are first assumed, and the wave functions are calculated. Improved charge distributions  $\rho_v(r_v)$  can

be evaluated using the wave function obtained. This process is repeated until self consistency is achieved.

### III. RESULTS

This section discusses the  $Ne_8$  and  $Ne_{13}$  clusters as the representatives of simple and face-centered cubic lattices [see Figs. 2(a) and 2(b)]. The basis functions used in all the calculations are from  $1s$  to  $3d$  atomic orbitals.

#### A. Compressed atomic neon

Using the basis functions generated from Eq. (2.1) with the well potential (2.2), an atomic neon has an electronic charge distribution only inside the well. If well radius is taken to be the ion-sphere radius  $R_0$ , the electron density  $\rho_e$  for this atom can be evaluated to be

$$\rho_e = 10 / \frac{4}{3} \pi R_0^3 .$$

The charge neutrality in an atomic region requires the atomic density  $\rho_n$  to be

$$\rho_n = \rho_e / 10 .$$

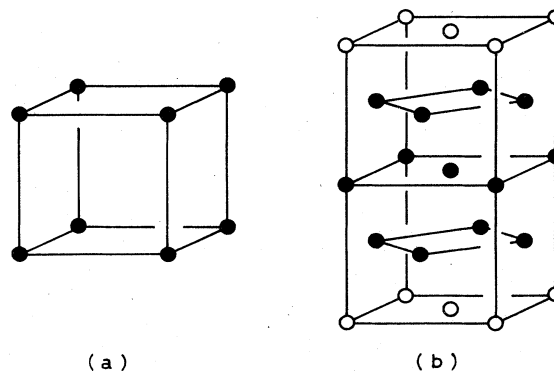


FIG. 2. Model clusters for high-density neon. (a) Simple cubic cluster  $Ne_8$ . (b) Face-centered-cubic cluster  $Ne_{13}$ . Open circles in (b) indicate the atomic sites outside the cluster considered.

Figures 3(a) and 3(b) illustrate the obtained atomic energies for larger and smaller  $R_0$  regions, respectively. Where  $R_0$  is larger than 2.0 a.u. ( $\rho_n$  is less than  $2 \times 10^{23}$  atoms/cm<sup>3</sup>), there is no difference between the present results and those for an isolated neon. As the atomic density increases the energy of the  $K$  shell goes up and reaches 190 eV at  $10^{26}$  atoms/cm<sup>3</sup>. The  $L$ - and  $M$ -shell orbitals also show a similar increase in their energies. The ener-

gies of  $s$ -type orbitals ( $l=0$ ) become larger than those of  $p$ - and  $d$ -type orbitals. In the smaller interionic region in Fig. 3(b) the orbital energies show the linear dependence in logarithmic scale upon the atomic distance.

## B. United-atom limit and simple cubic cluster of $\text{Ne}_8$

### 1. United-atom limit of $\text{Ne}_8$ (Hg)

A simple cubic cluster of neon in Fig. 1(a) becomes an Hg atom in the united-atom limit, provided it is an isolated cluster. Since this isolated cluster does not satisfy the condition of charge neutrality, it is not a suitable model for our present purpose. However, we have tried a calculation with this condition as a test of computer codes and for comparison with the following results.

Figure 4 plots the orbital energies of the  $\text{Ne}_8$  against the interatomic distance, the range of which is of interest in connection with the following discussion. The number of nondegenerate orbitals is 48. Orbital energies are calculated at interatomic distances 0.3, 0.5, 0.7, 1.0, 1.4, 2.0, 4.0, and 8.0 in a.u. The Lagrange interpolation of degree three connects them smoothly. As is expected, the  $2s$  and  $2p$  orbitals of the neon atoms mix with those of neighboring atoms as the interatomic distance decreases. Some of the bonding levels come down and approach the core orbitals of the Hg atom. On the contrary, antibondinglike levels gain their energy. Even the  $1s$  orbitals of the neon atoms mix with each other at distances smaller than 1.0 a.u. The energy shifts start from larger interatomic distances. The attractive potential from the eight neon atomic cores causes these shifts. Figure 5 illustrates the effective potential  $U_C + U_{ex}$  in the Hamiltonian [in Eq. (2.6)] at an interatomic distance 1.4 a.u. This potential is common to all one-electron molecular orbitals. We will discuss the meaning of this potential in Sec. III C.

At interatomic distances shorter than 0.02 a.u. the

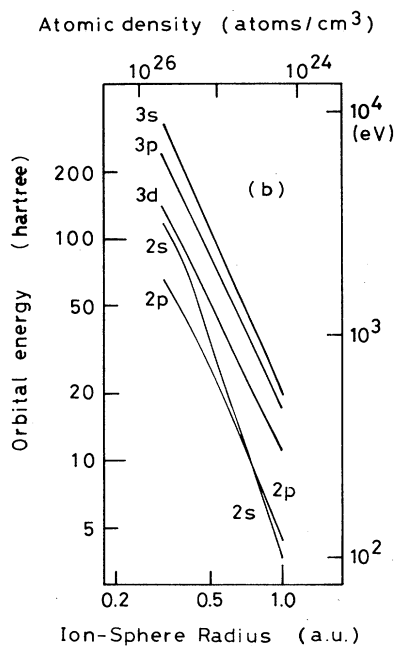
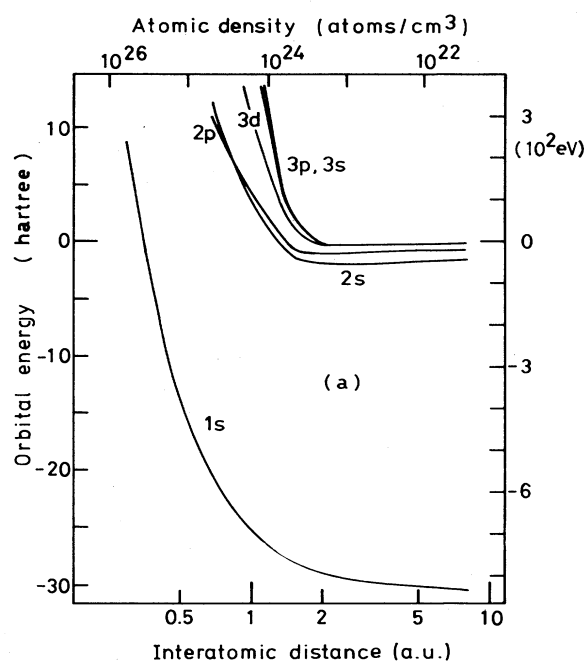


FIG. 3. Energy levels of atomic neon for various ion-sphere radius  $R_0$ . (a) Larger- $R_0$  region (i.e., low-density region) to a linear energy scale. (b) Smaller- $R_0$  region (i.e., high-density region) to a logarithmic energy scale.

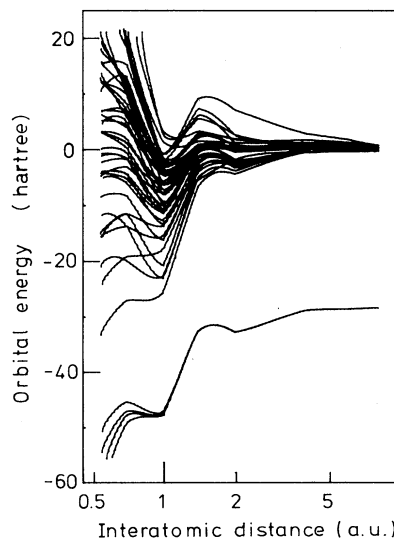


FIG. 4. Orbital energies for simple cubic cluster  $\text{Ne}_8$  vs the interatomic distance. Spatial spread of the wave function is not limited in this calculation.

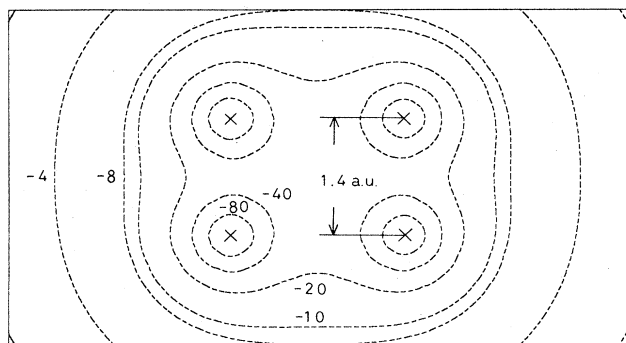


FIG. 5. The effective potential on an inclined plane which holds four Ne atoms. Contours shown are for  $-4.0$ ,  $-8.0$ ,  $-10.0$ ,  $-20.0$ ,  $-40.0$ , and  $-80.0$  hartrees at an interatomic distance of  $1.4$  a.u. Crosses indicate the positions of the atoms.

lowest orbital of the cluster is the bonding orbital of Ne  $1s$ . The energy of this orbital is about  $-80$  keV and approximately agrees with that of the Hg  $1s$  orbital (about  $-83$  keV).

## 2. Simple cubic cluster $Ne_8$

Now we return to the analysis of dense matter. The atomic density  $\rho_n$  of the cluster is

$$\rho_n = \frac{1}{d^3},$$

where  $d$  represents the interionic distance. If the electron density  $\rho_e$  is taken to be  $10\rho_n$ , the 80 electrons in a cluster must be localized within the volume  $(2d)^3$ . The shape of this volume, which may alter the electronic property of the cluster, is not known. Here we assume this volume to be  $A$ , the overlapping spheres each of which is centered on each atom (in Fig. 6) and  $B$ , a cube of a volume  $(2d)^3$ . The results for the  $B$ -type cluster will be presented at the end of this subsection.

Using the basis functions localized in a sphere of radius  $R_0$  ( $\cong 0.63d$ ), the charge neutrality is satisfied in our hypothesis. In the ion-sphere model, which is valid for  $\Gamma \gg 1$ , the electronic charge is localized within spheres

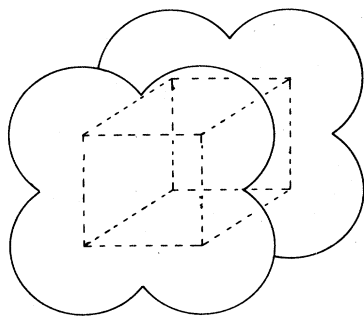


FIG. 6. Shape of overlapping spheres for  $Ne_8$ . Electronic charge is confined only inside the spheres.

which do not overlap each other. This model prevents atomic wave functions from mixing. On the other hand, the boundary condition  $B$  yields delocalized distribution of electrons. In model  $A$ , which lies in between these two extremes, the atomic orbitals can interact with each other within the cluster.

The calculated orbital energies for varying  $d$  are summarized in Table I and illustrated in Figs. 7(a) and 7(b) in linear and logarithmic energy scales, respectively. The calculation was performed at  $d=0.5, 0.7, 1.0, 1.2, 1.4, 2.0, 4.0$ , and  $8.0$  a.u.

As for the energies of the outermost bands of orbitals,

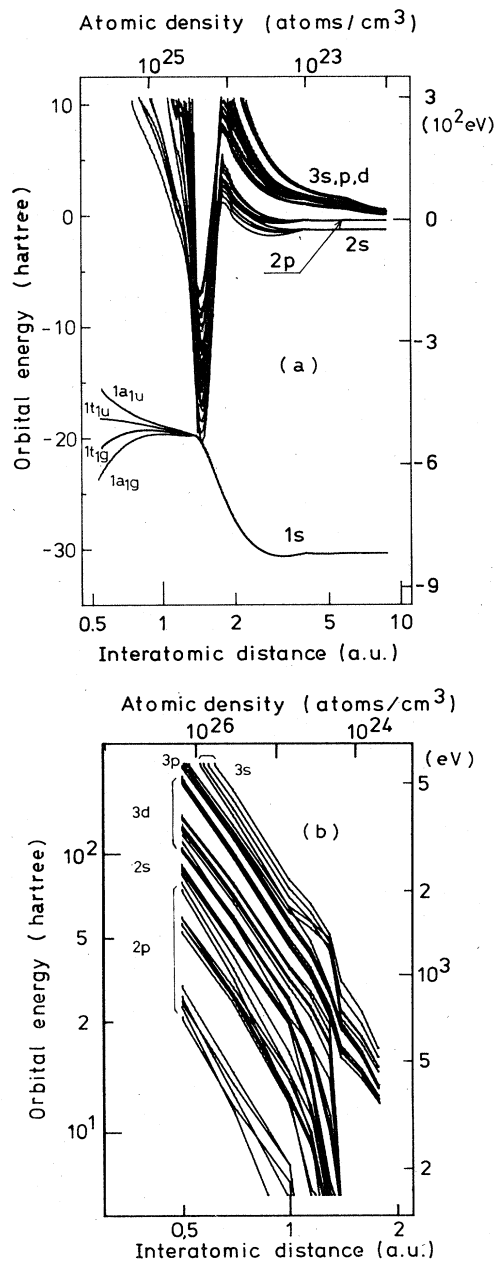


FIG. 7. Orbital energies for simple cubic neon cluster  $Ne_8$  for varying interionic distance  $R$ . (a) Low-density region. (b) High-density region.

TABLE I. Orbital energies for the Ne<sub>8</sub> cluster (in hartrees).

Level	Interionic distance (a.u.)							
	0.5	0.7	1.0	1.2	1.4	2.0	4.0	8.0
1a 1g	-50.43	-41.33	-39.29	-39.61	-39.58	-54.53	-60.69	-60.70
2a 1g	56.83	23.85	7.42	-10.59	-24.86	-0.28	-2.60	-2.58
3a 1g	148.70	71.42	25.94	-3.43	-16.94	3.33	-0.92	-0.93
4a 1g	177.24	96.63	49.06	10.03	-11.39	11.83	1.94	0.19
5a 1g	367.03	194.60	93.71	52.93	39.42	17.61	2.87	0.53
6a 1g	533.19	275.24	129.34	66.25	49.03	20.42	3.21	0.86
1eg	52.03	24.95	13.23	-9.44	-28.24	2.43	-0.92	-0.93
2eg	174.79	94.95	49.13	-1.61	-14.34	11.11	2.18	0.42
3eg	179.15	96.96	50.26	12.05	-11.50	12.03	2.98	0.79
4eg	361.97	193.88	94.21	52.11	37.21	18.25	3.28	0.83
1t 1g	-36.39	-36.95	-38.23	-39.36	-39.65	-54.43	-60.69	-60.70
2t 1g	67.49	32.93	15.25	-8.26	-32.22	1.57	-2.55	-2.58
3t 1g	112.55	61.15	26.53	8.90	-28.06	3.53	-0.90	-0.93
4t 1g	170.07	86.43	39.01	11.24	-21.92	5.07	-0.82	-0.93
5t 1g	211.09	120.46	60.24	23.03	-19.37	13.13	2.14	0.29
6t 1g	237.87	134.49	66.95	36.97	-14.60	14.00	3.12	0.54
7t 1g	249.76	139.54	71.02	41.22	-13.53	15.98	3.22	0.71
8t 1g	379.36	204.20	100.47	56.93	40.96	19.55	3.57	0.97
9t 1g	429.21	234.78	113.16	62.96	48.42	20.65	3.74	1.01
10t 1g	572.90	313.61	151.37	97.00	62.20	27.41	4.64	1.07
1t 1u	112.48	63.20	31.10	8.99	-31.05	4.74	-0.82	-0.93
2t 1u	210.77	117.33	61.34	20.82	-17.77	14.10	3.32	0.68
3t 1u	270.69	155.23	78.44	45.50	-16.62	16.73	3.45	0.94
4t 1u	434.31	241.62	123.98	93.71	51.54	25.02	4.86	1.26
1a 1u	-29.21	-34.85	-37.77	-39.20	-39.71	-54.43	-60.69	-60.70
2a 1u	118.67	63.22	27.54	9.47	-32.37	2.96	-2.52	-2.58
3a 1u	225.51	116.01	52.01	30.99	-23.64	5.55	-0.81	-0.93
4a 1u	246.64	141.77	72.26	41.59	-15.90	16.06	3.06	0.41
5a 1u	444.88	239.71	116.72	65.52	49.71	21.20	3.74	0.82
6a 1u	609.37	340.04	162.51	103.50	70.39	29.19	4.66	1.09
1eu	119.03	66.82	32.88	13.09	-33.24	4.95	-0.81	-0.93
2eu	245.01	141.34	71.96	42.17	-21.55	16.12	3.44	0.71
3eu	275.60	157.84	79.88	49.14	-17.62	17.28	3.78	1.07
4eu	456.80	253.50	129.93	99.68	54.54	25.95	4.96	1.27
1t 2u	59.34	30.02	15.21	-8.19	-29.39	2.69	-0.91	-0.93
2t 2u	181.26	99.11	51.27	12.98	-16.95	11.36	2.22	0.44
3t 2u	208.22	117.66	59.02	19.63	-12.29	13.92	3.23	0.82
4t 2u	369.34	198.85	97.06	54.08	38.99	18.97	3.46	0.95
1t 2g	-43.48	-39.13	-38.73	-39.50	-39.60	-54.43	-60.69	-60.70
2t 2g	61.88	27.61	11.39	-9.70	-30.21	0.72	-2.57	-2.58
3t 2g	105.69	58.47	25.58	-0.72	-25.64	3.47	-0.91	-0.93
4t 2g	158.18	77.93	33.22	5.74	-19.99	4.65	-0.82	-0.93
5t 2g	183.36	97.76	50.13	10.22	-15.49	12.09	2.03	0.23
6t 2g	206.11	115.54	60.65	20.11	-14.56	13.69	2.96	0.54
7t 2g	256.17	144.02	72.24	41.34	-12.29	14.61	3.16	0.66
8t 2g	372.86	198.75	97.20	54.62	39.79	18.58	3.21	0.84
9t 2g	413.33	227.41	111.48	62.87	47.17	20.27	3.49	0.95
10t 2g	548.81	291.23	140.88	90.56	55.21	25.59	4.65	1.12

their dependence on  $d$  can be classified into three categories. First, for  $d > 2.0$  a.u., the calculated orbital energies do not differ much from those of the atomic case. In this region the orbital energies gradually go up with the decreasing  $d$ . The energies of the  $1s$  orbitals increase with decreasing  $d$  down to about 1.5 a.u.; this behavior of  $1s$  energies is in contrast with the decreasing behavior for the Hg-like cluster stated in Sec. III B 1. The Coulomb repulsive interaction between the core and valence electrons makes this difference.

For  $1.0 < d < 2.0$  the valence orbitals of each atomic neon are mixed in a complicated manner and their energy levels diverge from each other. The lowering of the bottom of the  $2p$  band is noticeable in this region. The lowest orbital energy in the  $2p$  band is about  $-350$  eV at  $d = 1.4$  a.u. The Lagrange interpolation of orbital energies suggests the lowest  $2p$  energy to be about  $-600$  eV at 1.3 a.u. However, the calculation of the orbital at 1.3 a.u. turned out to be too difficult to obtain self-consistent results and we cannot determine an accurate value of the bottom of the valence band. The basis functions may not be suitable for the cluster at this interionic distance.

Finally, for  $d < 1.0$  a.u. the valence orbital energies show a dependence similar to the atomic case, though their levels diverge from each other by making bonding and antibonding orbitals. Their energies in logarithmic scale increase linearly with a decreasing interatomic distance.

A  $B$ -type cluster is calculated using basis functions prepared without the well potential in Eq. (2.2) and making the addition of a well potential at  $(2d)^3$  on the Hamiltonian. This potential selectively contributes to enhancement of the energies of wave functions which would have a large amplitude outside the cluster. In the variational procedure, electrons are filled in the orbitals which are located inside the cube and less affected by the additional potential. By modifying the Hamiltonian in this manner, spurious orbitals appear whose energies are decided in a rather arbitrary way. However, the obtained charge distribution is limited within the cube  $(2d)^3$ . As for the occupied levels, the  $B$ -type cluster makes the same results as those of  $A$ . This suggests that the electronic property is decided mainly by the position of the atoms and the volume in which electrons exist and is not sensitive to the spatial distribution of charges. Furthermore, truncated atomic basis functions are sufficient for representing the appropriate electronic charge density of the cluster.

### C. Face-centered-cubic neon cluster $\text{Ne}_{13}$

For the case of  $\text{Ne}_{13}$  cluster, illustrated in Fig. 2(b), the atomic density  $\rho_n$  is

$$\rho_n = \frac{\sqrt{2}}{d^3},$$

where  $d$  represents the distance between a pair of nearest-neighbor atoms. The requirement of charge neutrality determines the electronic density to be  $10\rho_n$ . In this calculation, we assumed that 130 electrons are located within the overlapping spheres with a radius of about  $0.79d$  and centered at the neon sites. The orbital energies obtained

for various interionic distances are tabulated in Table II and shown in Fig. 8. The overall features of the energy dependence on the density as the same as those of the  $\text{Ne}_8$  cluster. On the lower-density side, i.e., for  $d > 5.0$  a.u., the obtained results do not show a remarkable difference from that of the energies of isolated atom. Valence orbitals form band structures in the region of the interionic distance between 0.7 and 1.5 a.u. Because the  $\text{Ne}_{13}$  cluster is made of a larger number of atoms, the bandwidth is larger than that for the  $\text{Ne}_8$ . The energy difference between the valence band and the  $1s$  orbital becomes small at 1.4 a.u., and the bottom of the valence band is computed to be  $-600$  eV. The energy of the core orbital increases slightly with a decreasing  $d$  from 5.0 to 1.4 a.u. In the region of extremely small distances ( $d < 0.7$  a.u.), even the core orbitals make a band structure and levels repel each other. The valence orbitals exhibits a monotonical increase with the decreasing density.

Figure 9 shows the expectation values of the orbital radii against the interionic distance. The dashed line shows the well radii,  $0.79d$ . For  $d > 8.0$  a.u. the well potential does not affect the spread of the wave function. As the interionic distance decreases, the tails of the  $M$ -shell orbital become truncated at about 4.0 a.u., but they still overlap with the orbitals of the neighboring atoms. The orbital radii of  $2s$  and  $2p$  are about 0.7 a.u. in the case of an isolated atom. When the interionic distance diminishes to this extent, the energies of the  $L$  shell change drastically as shown in Fig. 8. If the atomic distance becomes much smaller than this normal size of the  $L$  shell, their energies increase monotonically. As for the  $1s$  orbitals, even the smallest interionic distance treated in this paper is not sufficiently short to compress them.

The effective potential in the Hamiltonian for the  $\text{Ne}_{13}$

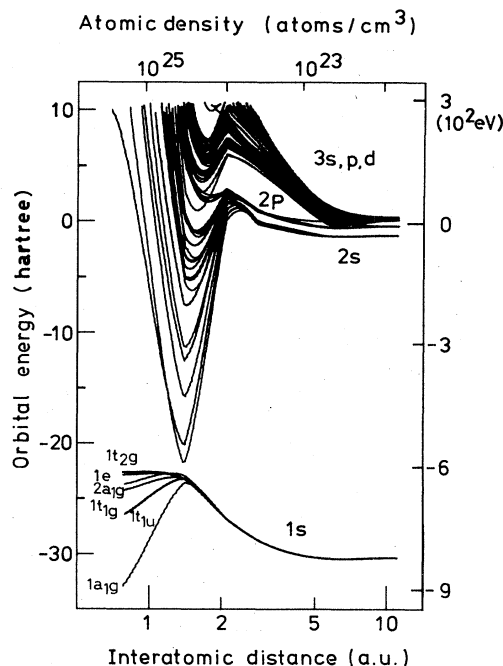


FIG. 8. Orbital energies for the face-centered-cubic cluster  $\text{Ne}_{13}$  against the distance of nearest-neighbor atoms.

TABLE II. Orbital energies for the Ne<sub>13</sub> cluster (in hartrees).

Interionic distance (a.u.)	0.4	1.0	1.5	2.0	4.0	8.0
Level						
1a 1g	-67.33	-47.17	-53.64	-57.27	-60.81	-60.67
2a 1g	-46.51	-45.75	-53.56	-57.23	-60.76	-60.61
3a 1g	26.59	-43.98	-0.09	-0.24	-2.75	-2.60
4a 1g	119.00	-10.98	3.06	0.11	-2.73	-2.60
5a 1g	133.27	1.84	4.88	1.87	-1.17	-0.92
6a 1g	177.57	15.86	13.57	10.19	-0.62	0.07
7a 1g	232.28	22.56	13.95	11.06	-0.11	0.14
8a 1g	329.51	27.58	17.78	12.50	0.83	0.32
9a 1g	475.24	31.55	23.85	16.67	1.08	0.50
10a 1g	592.92	77.99	30.98	17.25	1.51	0.54
1a 1u	104.56	11.21	5.41	2.18	-1.22	-0.92
2a 1u	220.75	24.72	17.10	12.75	1.34	0.36
3a 1u	406.39	57.12	25.47	17.79	2.31	0.65
1eg	-44.58	-46.35	-53.56	-57.27	-60.81	-60.67
2eg	56.87	-22.84	3.11	0.16	-2.75	-2.60
3eg	90.80	-6.33	4.41	1.91	-1.20	-0.92
4eg	137.08	1.04	5.38	2.10	-1.18	-0.92
5eg	180.86	16.98	13.18	10.16	-0.30	0.15
6eg	201.30	20.09	15.12	10.88	0.18	0.28
7eg	224.09	25.21	16.47	12.15	0.92	0.35
8eg	238.96	27.64	18.17	12.30	1.38	0.58
9eg	337.23	28.25	21.19	15.81	1.61	0.56
10eg	382.50	43.55	23.68	16.42	1.83	0.59
11eg	575.22	78.76	30.24	18.88	2.52	0.67
1t 1g	-47.70	-46.34	-53.56	-57.27	-60.81	-60.67
2t 1g	42.76	-31.89	2.02	0.06	-2.75	-2.60
3t 1g	78.94	-9.81	4.08	1.81	-1.20	-0.92
4t 1g	130.58	-4.07	4.94	2.03	-0.12	-0.92
5t 1g	148.40	5.59	11.71	9.20	-0.47	0.12
6t 1g	174.97	13.66	13.32	10.09	-0.00	0.26
7t 1g	199.47	21.06	13.90	10.30	0.49	0.32
8t 1g	223.01	23.19	16.22	11.65	0.88	0.45
9t 1g	248.66	25.21	18.37	11.87	1.35	0.52
10t 1g	343.09	29.44	20.95	14.50	1.42	0.53
11t 1g	380.08	48.77	23.74	16.15	2.16	0.61
12t 1g	546.16	78.53	29.02	18.02	2.83	0.71
1t 1u	73.76	-8.21	4.52	1.97	-1.21	-0.92
2t 1u	108.58	10.20	5.56	2.16	-1.12	-0.92
3t 1u	174.21	16.17	14.07	10.25	0.43	0.29
4t 1u	227.36	24.00	17.39	12.32	1.34	0.38
5t 1u	236.23	25.16	17.83	12.57	1.37	0.53
6t 1u	354.36	45.42	22.55	16.09	2.35	0.66
7t 1u	433.86	66.91	27.05	17.42	2.72	0.69
1a 1u	251.47	43.14	18.91	12.78	2.49	0.70
1a 2g	44.71	-25.02	3.06	1.76	-1.21	-0.92
2a 2g	165.21	11.04	12.00	9.17	-0.10	0.23
3a 2g	319.89	25.86	19.82	14.42	1.25	0.51
1eu	95.83	0.35	5.24	2.08	-1.20	-0.92
2eu	166.58	13.87	13.38	10.00	0.68	0.34
3eu	231.76	23.81	17.61	12.21	1.40	0.50
4eu	424.55	64.29	26.37	16.72	2.74	0.68

TABLE II. (Continued).

Interionic distance (a.u.)	0.4	1.0	1.5	2.0	4.0	8.0
Level						
1t2g	-44.02	-46.34	-53.56	-57.27	-60.81	-60.67
2t2g	82.64	-6.22	3.34	0.17	-2.74	-2.60
3t2g	96.97	-2.73	4.89	2.01	-1.21	-0.92
4t2g	156.37	12.96	5.44	2.14	-1.18	-0.92
5t2g	191.53	20.05	14.30	10.38	-0.22	0.15
6t2g	211.21	24.14	16.22	11.25	0.67	0.32
7t2g	216.98	26.03	16.52	12.11	1.31	0.37
8t2g	239.34	27.98	17.37	12.62	1.59	0.54
9t2g	360.99	30.81	23.20	16.11	1.64	0.57
10t2g	388.82	49.29	24.17	17.11	1.92	0.62
11t2g	563.56	68.54	29.46	18.66	2.32	0.66
1t2u	-52.72	-46.37	-53.56	-57.27	-60.81	-60.67
2t2u	13.81	-40.59	1.01	-0.49	-2.75	-2.60
3t2u	61.75	-15.16	3.78	1.75	-1.21	-0.92
4t2u	86.64	-10.04	4.11	1.89	-1.20	-0.92
5t2u	103.62	0.54	5.13	2.05	-1.19	-0.92
6t2u	147.98	11.60	5.75	2.15	-1.15	-0.92
7t2u	167.76	15.01	13.30	9.95	-0.60	0.10
8t2u	183.92	19.78	13.85	10.43	-0.11	0.25
9t2u	192.32	21.43	14.60	10.88	0.21	0.27
10t2u	221.80	23.04	16.29	11.59	0.82	0.33
11t2u	304.45	25.70	18.89	13.59	1.26	0.39
12t2u	329.20	26.12	20.64	15.32	1.29	0.52
13t2u	395.11	30.39	23.35	16.04	1.39	0.54
14t2u	429.16	56.46	25.77	16.56	2.32	0.59
15t2u	540.37	82.29	29.86	18.00	2.62	0.63

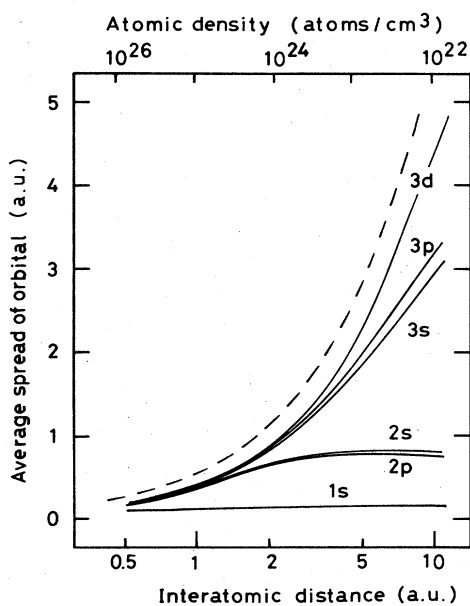


FIG. 9. Average orbital spread ( $\langle r \rangle$ ) used for the  $\text{Ne}_{13}$  cluster calculations. Dashed curve indicates an upper bound owing to the truncation of the wave functions in advance. For details see text.

cluster at an interionic distance 1.4 a.u. is shown in Fig. 10. It is greatly different from the effective potential for the Hg-like  $\text{Ne}_8$  cluster in Fig. 5. In the case of  $\text{Ne}_8$  the potential gradually becomes deeper as the distance from the atomic core becomes small, but the potential for the

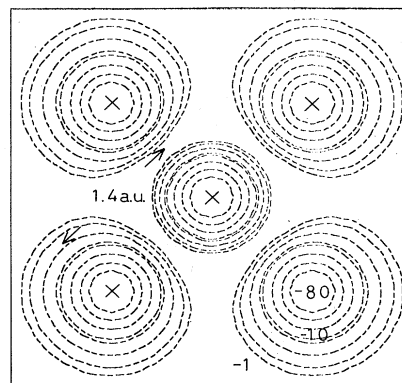


FIG. 10. Effective potential for the  $\text{Ne}_{13}$  cluster calculation on a horizontal plane which holds the central atoms. Contours of  $-1.0$ ,  $-2.0$ ,  $-4.0$ ,  $-8.0$ ,  $-10.0$ ,  $-20.0$ ,  $-40.0$ , and  $-80.0$  hartrees are shown. The distance of nearest-neighbor atoms is 1.4 a.u. Crosses indicate the positions of atoms.

Ne<sub>13</sub> cluster goes down suddenly near the atomic core and is almost flat between atoms.

#### IV. DISCUSSION

The electronic properties of highly compressed matter studied in the present work can be stated in four points.

The first characteristic of highly compressed matter is the large magnitude of the kinetic energy of electrons. This can clearly be seen in the results for the atomic neon. The wave function employed here has an amplitude only in the well potential. This makes valence orbital energies increase with decreasing  $R_0$ . Since the energy of a state in a spherical well potential is proportional to the inverse of the square of  $R_0$ , it is natural that the orbital energies show a linear dependence on  $R_0$  on a log-log scale.

The second feature is the growth of the  $1s$  orbital energy as  $R_0$  becomes small. This cannot be explained by the confinement of the  $1s$  wave function into the well potential. Since the mean orbital spread  $\langle r \rangle$  for the  $1s$  orbital of the neon atom is about 0.1 a.u., the applied potential barrier does not alter the spatial size of this orbital nor its kinetic energy. The increase of the  $1s$  energy is attributed to the repulsive interaction between the electrons, which changes the screening charge. For  $R_0$  smaller than 0.5 a.u. the charge does not distribute as an isolated atom. Since the valence orbital wave functions are sine-wave-like, charge distribution becomes uniform. Electrons concentrated near the nuclei make the attractive potential small for  $1s$  orbital. This change in the amount of charge screening for the core orbital explains the second feature.

The third feature is characteristic of the cluster calculation. When neon atoms come together, the valence orbitals of the atomic neons make bonding and antibonding molecular orbitals and form a bandlike structure. This effect is superposed on the increase of the energy owing to the confinement of the wave functions (the first feature). The lowering of the energy by making a bonding orbital is thought to be smaller than the increase of the kinetic energy by compression, because the orbital energies for the Ne<sub>8</sub> and Ne<sub>13</sub> clusters at  $R_0 > 2.0$  a.u. incline toward the higher-energy side.

The fourth feature is the lowering of the bottom of the valence band at 1.4 a.u. As the interionic distance decreases, the valence electrons of the neon atom are affected by the attractive Coulomb potentials not only from the nucleus belonging to the same atom but also from the neighboring nuclei. The steep lowering of the  $2s$  and  $2p$  bands seems to occur when the average radii of these orbitals match the interionic distance. In other words, these orbitals have large amplitudes at the position of the neighboring atom cores. As shown in Fig. 9, the effective potential for the Ne<sub>13</sub> cluster at  $d=1.4$  a.u. is thought to be of a short-range type. The inner-core orbitals gain their energy because of the large effective screening charge, as mentioned in relation to the second feature. As the interionic distance approaches 1.4 a.u., these orbitals are squeezed up to the shoulder of the potential. On the other hand, the valence electrons move around every atomic site and lower their energies. Therefore, the difference be-

tween the energies of valence and core orbitals becomes small.

Kishimoto and Mima<sup>7</sup> applied the tight-binding approximation to disordered materials and estimated the width of the  $2p$  band of the Ne<sup>+9</sup> ion up to a density of about 100 g/cm<sup>3</sup> (i.e.,  $3.0 \times 10^{24}$  atoms/cm<sup>3</sup>). The result depends upon the atomic potential used for their calculation (i.e., the strength of the perturbation). The obtained values for the  $2p$  bandwidth are about 450 and 120 eV at 60 g/cm<sup>3</sup> (i.e.,  $1.8 \times 10^{24}$  atoms/cm<sup>3</sup>) for the Coulomb potential and the ion-sphere potential, respectively. Our present result for the Ne<sub>13</sub> cluster is 360 eV and is in between their two values. This reflects the fact that the obtained effective potential in our calculation is a mixture of Coulomb and ion-sphere potentials. As mentioned in Sec. II, we do not suppose any shape of the atomic potential in the calculation, except the additive well potential which is used to fulfill the requirement of charge neutrality. Then the potential is originally Coulombic and the interaction between electrons automatically adds the feature of an ion-sphere potential as the interionic distance becomes small.

When the interionic distance becomes zero, our present model ends up with a united atom in the well potential of infinite height. The results obtained for the clusters at  $R_0 < 0.5$  a.u. are nearly the same as those for the united atom. The density corresponding to  $R_0=0.5$  a.u. is about 1000 times of a usual solid. Though the valence orbitals form the band structure and broadened energy levels of the united atom, the features obtained cannot be an accurate representation of the electronic property. The enlargement of clusters and the addition of basis orbitals for continuum wave functions may improve the results.

In a relatively low-density region the obtained results may not be accurate either. Gupta and Rajagopal<sup>5</sup> estimated that the level shifts of the inner core for the densities from  $1.0 \times 10^{23}$  to  $4.54 \times 10^{23}$  atoms/cm<sup>3</sup> are 127 and 71 eV at  $T=100$  and 700 eV, respectively. The value obtained for the Ne<sub>13</sub> cluster is about 50 eV in our calculation and is about half of their values. The interionic distance in question is 3.0–1.7 a.u. and the density is about a few times that of a usual solid; i.e., it is outside the region of our interest. For a precise calculation in this density region accurate potential and wave functions outside the clusters may be needed. The contribution from thermal ionization also should be taken into account.

#### V. SUMMARY

The DV- $X\alpha$  cluster method is a useful approach for the analysis of the electronic properties of extremely high-density plasma. Assuming clusters of small size, we have applied this method to the neon plasma at zero temperature.

As mentioned in Sec. IV, the present results do not agree well with those obtained by effective potential methods for intermediate-density plasma. This discrepancy is due mainly to the omission of the thermal fluctuation from neutrality in the cluster. When the Debye radius  $R_D$  is larger than the ion-sphere radius, a knowledge of the delocalized electron wave function is indispensable.

This requirement cannot be achieved in our present models for the intermediate-density plasma.

We believe that the DV- $X\alpha$  method can be applied to an arbitrary electron temperature by considering free or excited orbitals and assuming the Fermi distribution for the electron population. As a matter of fact, these orbi-

tals are obtained in the present calculations as antibondinglike orbitals whose occupation numbers equal zero. However, the propriety of substituting continuum wave function for discrete ones should be checked. We are working in this direction and the results for an arbitrary electron temperature will be presented in the near future.

- 
- <sup>1</sup>S. G. Brush, H. L. Sahlin, and E. Teller, *J. Chem. Phys.* **45**, 2102 (1966).  
<sup>2</sup>J. C. Stewart and K. D. Pyatt, Jr., *Astrophys. J.* **144**, 1203 (1965).  
<sup>3</sup>S. Skupsky, *Phys. Rev. A* **21**, 1316 (1979).  
<sup>4</sup>U. Gupta and A. K. Rajagopal, *J. Phys. B* **22**, L704 (1979).  
<sup>5</sup>U. Gupta and A. K. Rajagopal, *J. Phys. B* **14**, 2309 (1981).  
<sup>6</sup>W. Zakowicz, I. J. Feng, and R. H. Pratt, *J. Quant. Spectrosc. Radiat. Transfer* **27**, 329 (1982).  
<sup>7</sup>Y. Kishimoto, K. Mima, and Y. Kato, in *Proceedings of the Conference and Workshop on Radiative Properties of Hot Dense Matter, 1983* [*J. Quant. Spectrosc. Radiat. Transfer* (to be published)].

- <sup>8</sup>B. Fricke *et al.*, *Phys. Lett.* **5**, 375 (1976).  
<sup>9</sup>B. Yaakobi *et al.*, *Phys. Rev. A* **19**, 1247 (1979); N. Miyanaga, Y. Inada, and Y. Kawai, *Annual Progress Report on Laser Fusion Program, 1979* (Institute of Laser Fusion Engineering, Osaka University, Osaka, unpublished).  
<sup>10</sup>H. Iyetomi and S. Ichimaru, *Phys. Rev. A* **27**, 3241 (1983); S. Ichimaru, *Rev. Mod. Phys.* **54**, 1107 (1982).  
<sup>11</sup>H. Adachi, M. Tsukada, and C. Satoko, *J. Phys. Soc. Jpn.* **3**, 875 (1976).  
<sup>12</sup>A. Rosen *et al.*, *Chem. Phys.* **65**, 3085 (1976).  
<sup>13</sup>J. C. Slater, *Quantum Theory of Molecules and Solids* (McGraw-Hill, New York, 1974), Vol. 4.